Iron ores in the Fen central complex, Telemark (S. Norway): Petrography, chemical evolution and conditions of equilibrium

TOM ANDERSEN

Andersen, T.: Iron ores in the Fen central complex, Telemark (S. Norway): Petrography, chemical evolution and conditions of equilibrium. *Norsk Geologisk Tidsskrift,* Vol. 63, pp. 73–82. Oslo 1983. ISSN 0029-196X.

Hydrothermal iron ores from the Fen central complex may be classified according to their mineral assemblages as primary (magnetite ± pyrite ± anatase + calcite) or secondary (hematite ± goethite + calcite ± dolomite). Primary ores equilibrated between the hematite – magnetite and magnetite – pyrite – pyrrhotite buffers, at temperatures below 600°C. Alteration to form the secondary parageneses took place above the hematite – magnetite buffer, probably at lower temperatures.

T. Andersen, Department of Geology, University of Oslo, Box 1047, Blindern, Oslo 3, Norway.

The Fen central complex (Brøgger 1921, Sæther 1957, Barth & Ramberg 1966) is an early Cambrian alkaline intrusive complex, situated 119 km S. W. of Oslo, ca. 20 km W of the late Paleozoic Oslo Rift (Fig. 1). The intrusive rocks range in composition from alkaline lamprophyres ('*damtjernite*') and rocks of the urthite-ijolite-melteigite association, to calcite carbonatite (*søvite*), dolomite carbonatite (*rauhaugite I*) and ankerite-ferrocarbonatite (*rauhaugite II*). They have penetrated Precambrian granitic gneisses, which are fenitized along the western margin of the central complex.

Iron ores associated with the carbonatites were worked from the mid-seventeenth century until 1927 (Vogt 1918, Bjørlykke & Svinndal 1960). Vogt (1918) estimated the production during this period to one million tons of ore, with present reserves of the same order of magnitude. Mining took place at several localities in and around the central complex. The most extensive workings were in the Gruveåsen area, close to the eastern margin of the complex, where operations by the 1920's had reached a level 225 m below the surface of lake Norsjø.

The Fen iron ores are typically veins, lenses or dyke-like bodies, found within carbonatites or in carbonated gneisses in their immediate surroundings. (Sæther 1957). They are most frequently associated with rauhaugite II or metasomatized hematite-dolomite-calcite carbonatite (*rødberg*) in the central and eastern parts of the complex. Isolated orebodies in søvite or rauhaugite I are also known.

The orebodies range in width from a few centimetres to 2–3 metres, and may extend some tens of metres along strike. Because of thick cover and extensive mining, few surface exposures are found in the central Gruveåsen area. A northwest-trending en-échelon structural pattern may nevertheless be deduced from the distribution of pits.

Vogt (1918), Brøgger (1921) and Sæther (1957) interpreted the iron ores as metasomatically introduced, and connected their actual emplacement to the development of the rødberg. Sæther (1957, p. 118) noted the presence of magnetite and pyrite in some of the Fen hematite ores, without attaching any petrogenetic significance to the observation. However, recent results (Andersen 1982) indicate that the rødberg was formed essentially by oxidation and partial dissolution of older magnetite- and pyrite-bearing rauhaugite II. These findings remove the necessity of postulating the introduction of ferric iron.

A petrographic reexamination of the Fen iron ores was therefore considered necessary, to check whether the ores follow the same post-emplacement evolutionary pattern as the carbonatite host rocks, and as far as possible to define the conditions of formation of the ores. The mineralogy of a multicomponent system, such as an iron ore, is controlled by several,

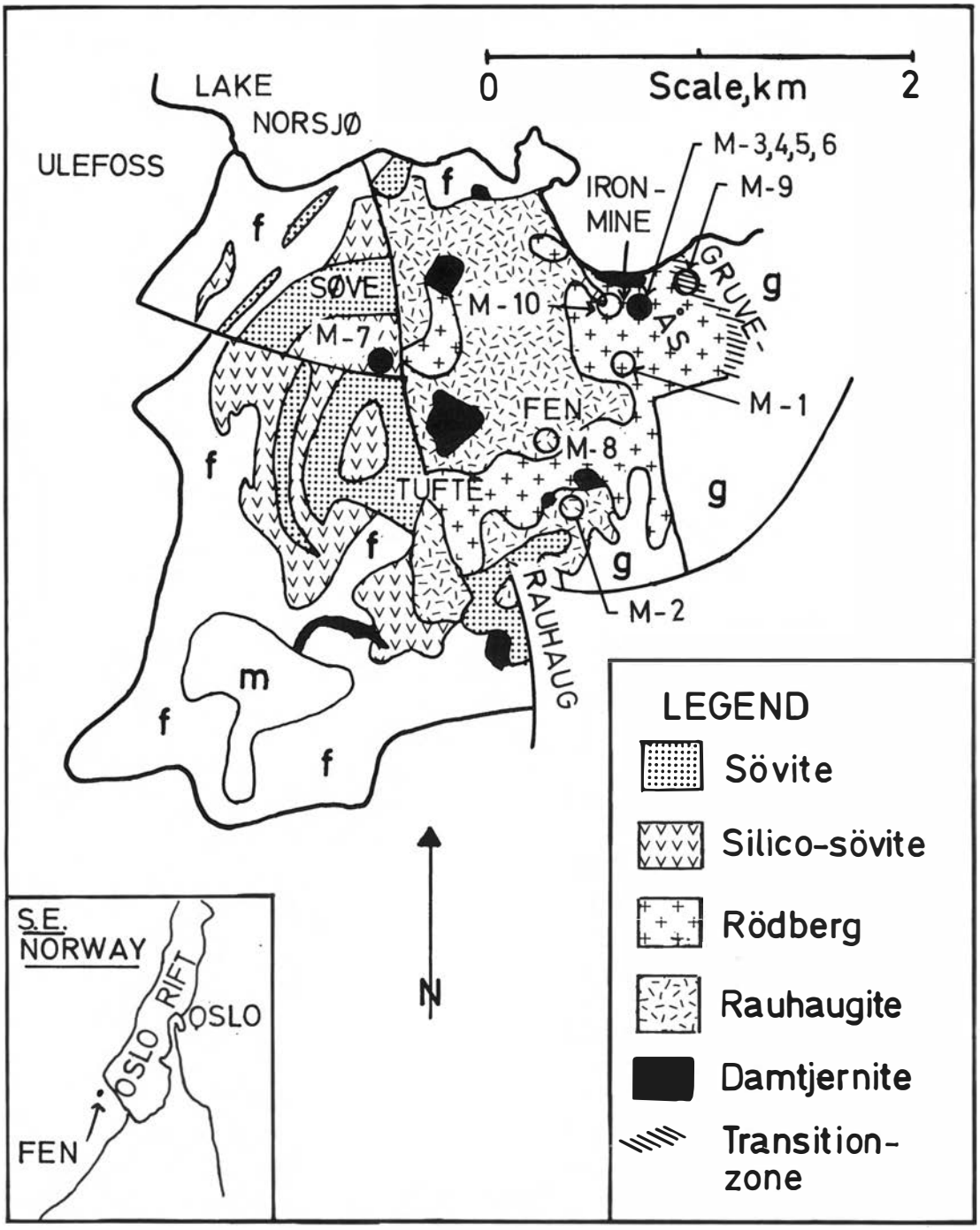

Fig. 1. Geological map of the Fen central complex, simplified from Dahlgren (1978), showing major carbonatite units and sample locations. Closed circles indicate underground samples. m: Melteigite and ijolitic rocks, f: Fenite, g: Gneiss.

Table 1. Opaque mineralogy of Fen iron ores. Samples M-7, 9, 10 were collected by the author, the others are from the W. C. Brøgger collection of the Mineralogical-Geological Museum, Oslo.

	Magnetite	Hematite	Pyrite	Maghemite	Goethite	Anatase	Locality	Hostrock
Magnetite ore								
M-5	M	m	m			m	Fen iron mines	Unknown
M-7	M	m	M	m	m		Tufte	Søvite and ranhaugite I
M-8	M	m			m		Fen	Rauhaugite II
Massive hematite ore								
M-1	(m)	M		m			S Gruveås	Rødberg
M-3	(m)	M	(m)				Fen iron mines	Rødberg
M-4	P	M					Fen iron mines	Rødberg
M-6	(M)	M		m			Fen iron mines	Rødberg
Disseminated hematite ore								
M-2	P	M	(m)			a	Rauhaug	Rødberg
M-9	P	M			M		E Gruveås	Rødberg and gneiss
M-10	P	M					NW Gruveås	Rødberg

Abbreviations: M: major phase, m: minor phase, a: accessory phase
P: pseudomorphs
( ) Unstable as judged from microstructures, but present in indicated amounts
– (underlined): phases in primary equilibrium.

more or less interdependent parameters (temperature, pressure, volatile fugacities, pH of coexisting solutions, activities of dissolved species). Quantification (at least within wide limits) and evaluation of the relative importance of these factors are needed to understand the chemical and mineralogical evolution of the ores.

The samples

Field study and sampling of Fen iron ores is made exceedingly difficult by thick Quaternary cover in most of the interesting area, and by the very extensive mining-operations, which have removed the near-surface parts of most major ore bodies. The existing surface exposures of both ore and carbonatite are also generally deeply weathered. The underground workings of the Fen iron mines are at present not accessible. Only three of the present samples were collected by the author (M-7, M-9, M-10), the remaining were taken from the W. C. Brøgger collection in the Mineralogical-Geological Museum, Oslo. All samples are fresh and unweathered, and were selected to cover a maximum range of petrographic variations.

With the exceptions stated, field relations are therefore unknown, and the hostrocks indicated in Table 1 have been interpreted from the map of Sæther (1957). All samples were studied by reflection microscopy of polished sections, using oil immersion and magnifications up to 400×. Phase-identifications were confirmed with the electron microprobe.

Carbonates were classified by cathodoluminescence as calcite (orange luminescence), dolomite (red) or ankerite (including parankerite; no luminescence).

Petrography

Petrographic relations of the individual samples are summarized in Table 1.

The ores, according to modal abundances, may be classified as either hematite or magnetite ore. For the hematite ore a further subdivision in massive and disseminated varieties is justified. Common to all Fen iron ores is the presence of quartz, chlorite and calcite; these phases occur as a fine-grained groundmass in the disseminated hematite ore, and as minor interstitial phases in the massive ores. Crosscutting calcite-veins are also frequently found.

As is seen from Table 1, the hematite ores generally seem to be associated with rødberg, whereas the magnetite ores are found in rauhaugite and søvite. Where field relations can be observed, hematite ores grade into their wall rocks, while magnetite ores seem to have sharp contacts.

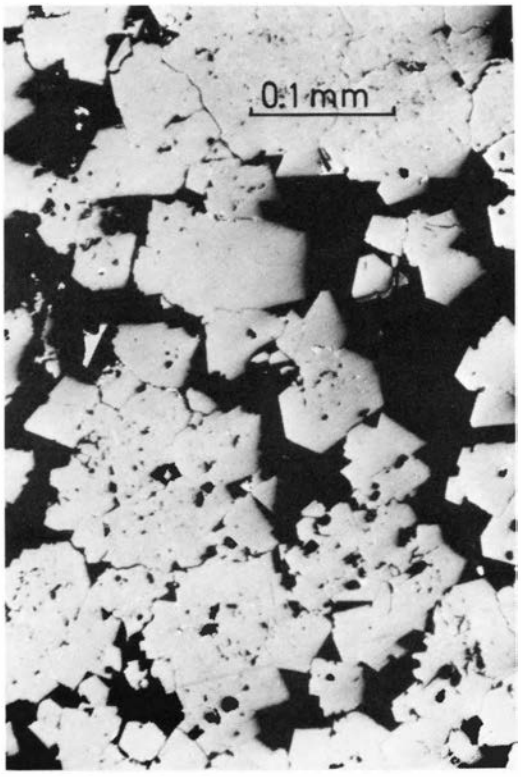

a

Fig. 2. Reflected light photomicrographs of Fen iron ores, plane polarized light and oil immersion.

a: Primary magnetite ore, sample M-5. Unaltered magnetite crystals (light grey) show octahedral outlines towards quartz and calcite (black). Small amounts of pyrite (white) are present.

b: Secondary hematite ore, sample M-4. Magnetite is totally replaced by hematite, which has grown as sets of semi-parallel, tabular crystals along (111) lamellae of the magnetite. The octahedral crystal habit has been retained during formation of the pseudomorphs.

The differences in reflectivity are caused by different orientation of individual hematite lamellae.

c: Incipient oxidation of magnetite, sample M-8.

Massive magnetite (grey) is showing signs of incipient oxidation, with hematite (white), developing as plates along the (111) direction of the magnetite.

d: Relics of magnetite in hematite ore, sample M-3.

This magnetite (mt) is replaced by hematite (hm), which has grown both along the margins of the resorbed crystals, and internally along the (111) direction.

e: Intergrowths of pyrite and magnetite in primary magnetite ore, sample M-7. Magnetite (mt) and pyrite (py) have crystallized together, and have only been affected by minor hematitization and later supergene alteration. Black: quartz and carbonates.

f: Resorbed and partly hematitized pyrite in disseminated hematite ore, sample M-2. Hematite (hm) has formed along the margin of the rounded pyrite (py), which is preserved in a small carbonate patch in the ore. Crystallites of hematite (white) are also scattered throughout the carbonate. The blurring of the crystal outlines against the groundmass is due to reflections from planes below the surface of the semi-transparent carbonate.

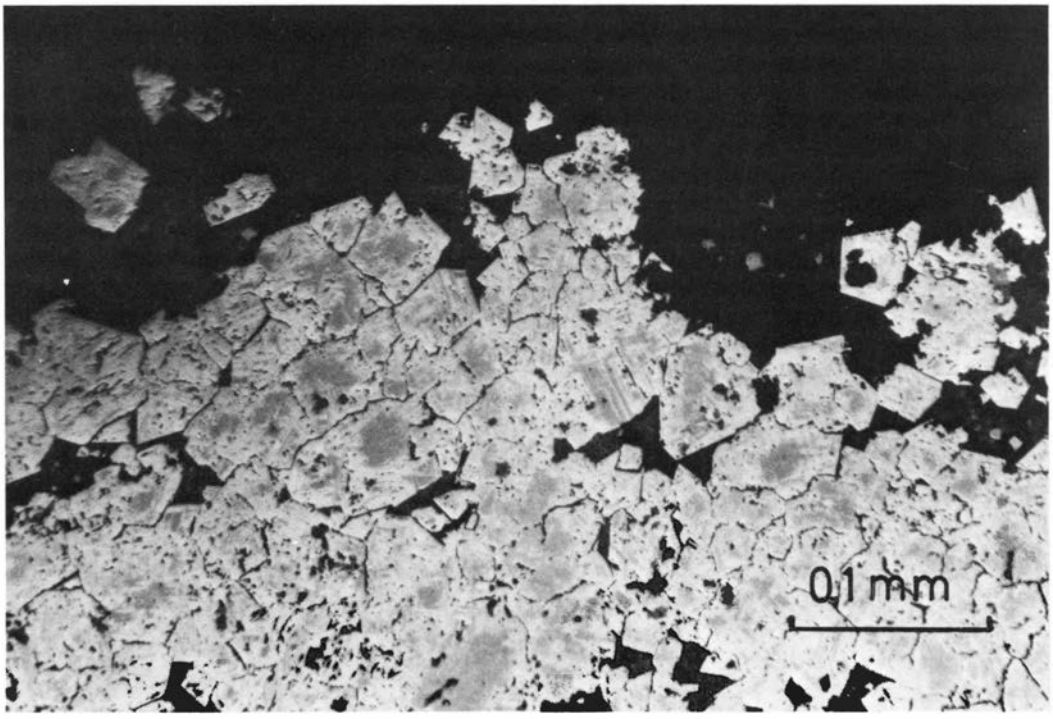

b

c

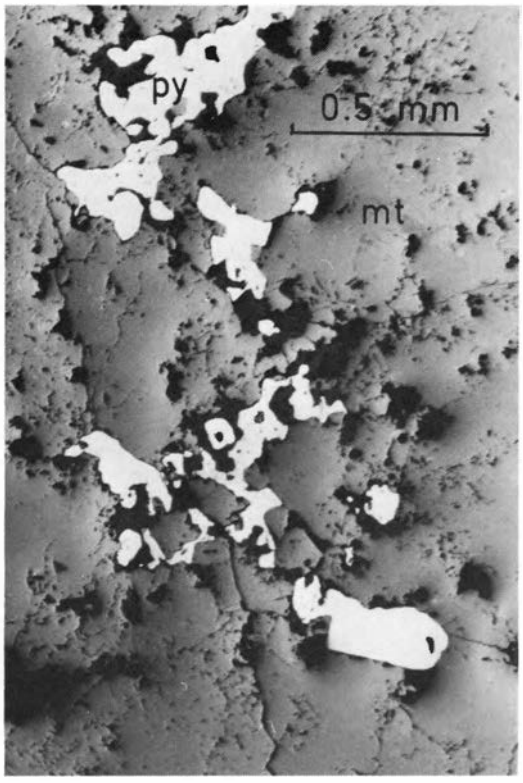

e

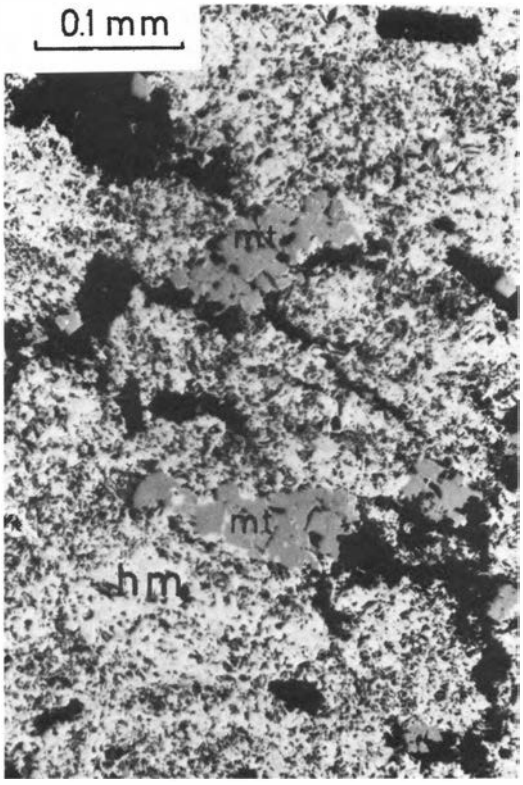

d

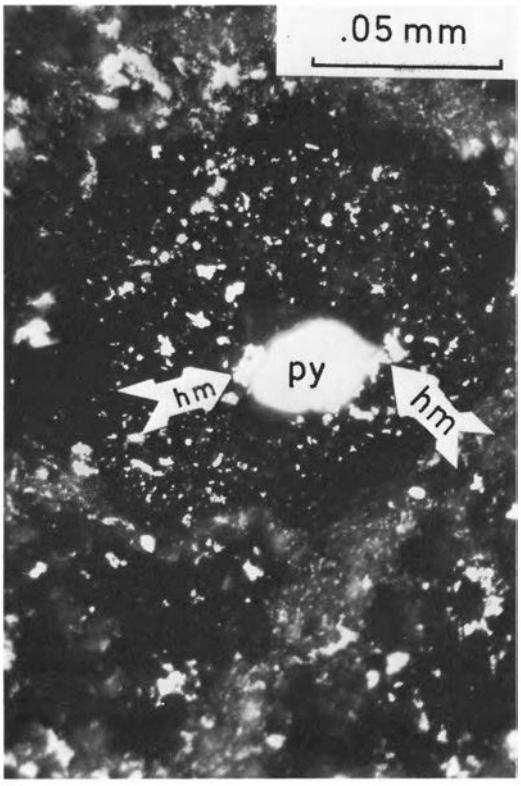

f

Table 2. Composition of magnetites from Fen iron ores; Wt % oxides. Means of three homogeneous grains in each sample. The analyses were made using the ARL–EMX electron microprobe of the Mineralogical-Geological Museum, University of Oslo equipped with a LINK energy-dispersive analyser unit. Structural formulae and ferric iron were calculated on a basis of 3.000 cations and 4.000 oxygens by the method of Neumann (1976).

	M-7	M-8
SiO_2	0.30	1.07
Al_2O_3	0.15	0.25
TiO_2	0.00	0.16
Fe_2O_3	67.14	65.19
MgO	0.38	0.28
FeO	30.46	31.83
MnO	0.06	0.04
Sum	98.39	98.82
Structural formula		
Si	0.011	0.042
Al	0.007	0.012
Ti	0.000	0.004
Fe^{3+}	1.971	1.896
Mg	0.016	0.016
Fe^{2+}	0.993	1.029
Mn	0.002	0.001

Magnetite ore

The samples are dominated by magnetite, with pyrite ranging from 0 to 15 %. The magnetite crystals have octahedral outlines toward matrix and interstitial calcite and quartz (Fig. 2a), and are partially oxidized to hematite along grain boundaries and (111) lamellae (Fig. 2c).

Minor amounts of secondary goethite and maghemite (identified by qualitative electron microprobe analyses and optical properties (Uytenbogaardt & Burke 1971)) postdate hematite, and are most probably very late (supergeneous?) alteration products unrelated to the major ore-evolution at Fen.

The magnetite is nearly stoichiometric (Table 2) with Ti-contents below those reported by Prins (1972) from carbonatites.

Pyrite is a primary phase, coexisting with magnetite in two of the samples studied (Fig. 2e). Anatase (Nb-bearing) and bastnäsite group minerals are accessories.

Massive hematite ore

Massive hematite ore is, in terms of volume, the most important ore-type of the Fen complex (Vogt 1918, Brøgger 1921). Hematite forms various massive sheaf-like aggregates, or more open grids of platy sub- to euhedral crystals, with interstitial quartz and minor calcite.

Magnetite is found only as relics (Fig. 2d), showing alteration to hematite along grain boundaries and (111)-lamellae. The replacement commonly has gone to completion, leaving martitic pseudomorphs or hematite aggregates with octahedral outlines as evidence of the former presence of magnetite (Fig. 2b).

Minor amounts of pyrite, partly replaced by hematite, are found in the 'grid-structured' variety.

Disseminated hematite ore

The disseminated hematite ore is petrographically intermediate between rødberg and massive hematite ore.

Martite pseudomorphs are scattered throughout an aphanitic matrix of hematite, calcite and iron-free dolomite, with frequent laths of chlorite. Hematite also occurs as laths embedded in goethite in mm-thick veins cutting this groundmass. (Goethite is, however, absent from M-10, which is taken from a 15 cm thick hematite-rich vein grading into ordinary rødberg.)

Small pyrite-relics (partly replaced by hematite) are scattered throughout the groundmass (Fig. 2f).

Anatase, apatite and monazite are accessory phases.

Discussion of results

Primary and secondary mineral assemblages

The primary phases of Fen iron ores, as seen from the petrographic relations outlined above, are magnetite, pyrite and in some samples also anatase.

These are replaced by hematite, with or without early formed goethite. In addition, small amounts of maghemite and goethite have been formed in some of the otherwise unaltered magnetite ores; this is a result of late (probably supergene) oxidation, which will not be considered further here.

Temperature and oxygen fugacity considerations

It is not possible to make any unique estimates of temperature of formation for the primary (mag-

netite-bearing) or secondary (hematite-bearing) mineral assemblages of the Fen iron ores. However, the occurrence of the ores as veins cutting carbonatite suggests primary introduction by hydrothermal solutions at temperatures below the solidus of the host carbonatite.

In broadly similar experimental systems this solidus lies in the interval 625 to 650°C (Wyllie 1966) at pressures below 1 kbar, which correspond to the shallow level of intrusion deduced by Sæther (1957).

Equilibration below 600°C is also indicated by the primary Ti-free magnetite + anatase assemblages found in samples M-2 and M-5. At higher temperatures increased magnetite-ulvøspinel solid solubility would stabilize titanomagnetite, coexisting with a TiO_2-phase or ilmenite solid-solution, depending on the oxygen fugacity (Lindsley 1976).

Siderite is a common low-temperature phase in iron-bearing carbonate rocks, including ferrocarbonatites (French 1971, Heinrich 1966). In the Fen complex siderite is absent from both carbonatites (Sæther 1957) and ores, whereas calcite and iron oxides always appear to be stable together. This suggests that final equilibration, both of the ores and their wallrocks, took place at temperature/oxygen fugacity-conditions above the siderite stability field, the upper limits of which are defined by the reactions:

(a): $3\ FeCO_3 + 1/2\ O_2 = Fe_3O_4 + 3\ CO_2$ below the hematite-magnetite buffer and

(b): $2\ FeCO_3 + 1/2\ O_2 = Fe_2O_3 + 2\ CO_2$ above the buffer, according to French (1971).

Under hydrothermal conditions, these reactions are rather insensitive to changes in total pressure, but depend heavily on the partial pressure of CO_2. The high T-f_{O_2} limit of the siderite field is therefore shown at three different P_{CO_2}, at a total pressure of 100 bar in Fig. 3 (thermodynamic calculations are given in the appendix). Accurate estimates of P_{CO_2} are not possible from the present data.

The oxygen fugacity of the primary magnetite-bearing assemblages is constrained to a rather narrow field in the T-f_{O_2} plane, by the magnetite-hematite and magnetite-pyrite-pyrrhotite buffers (Fig. 3 and appendix). At lower oxygen fugacities pyrrhotite-pyrite or pyrrhotite-magnetite bearing assemblages become stable, depending on f_{S_2} and the pH of the system.

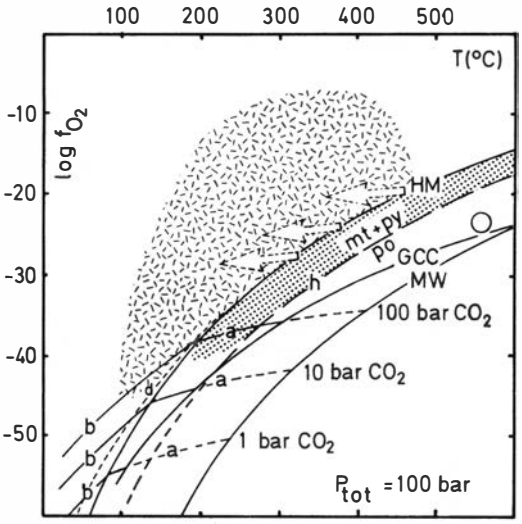

Fig. 3. Approximate temperature-oxygen fugacity fields of primary (dotted) and secondary (hachured) iron ore equilibrium at Fen.

HM: Hematite-magnetite buffer, GCC: Graphite-CO-CO_2 buffer,
MW: Magnetite-wustite buffer. (abbreviations according to Wones & Gilbert 1982).

Derivation of oxygen buffer curves and stability limits is discussed in the appendix. All curves are calculated at an (arbitrarily chosen) total pressure of 100 bar, corresponding to a depth of 1 km in a hydrothermal system. Small letters on curves refer to equilibria discussed in the text and the appendix.

The sets of parallel curves limiting the stability field of siderite refer to partial pressures of CO_2 equal to 100, 10 and 1 bar respectively.

Curve (d) is the T-f_{O_2} locus of equal activities of H_2S and HSO_4^-, calculated at pH buffered by calcite ($a_{Ca}^{2+} = 10^{-2}$ molar, $P_{CO_2} = 10$ bar) Sources of thermodynamic data are listed in the appendix.

The maximum f_{O_2} and the minimum temperature of the equilibration field for the secondary ores are undetermined. The exact positions of the limits toward the siderite stability field depend on the CO_2 pressure, and are therefore drawn irregularly.

Stippled arrows are possible (but not unique) paths for evolution of the ores from the primary to the secondary T–f_{O_2} fields.

The open circle (T = 560°C, log f_{O_2} = –23.5) represents the point of final equilibration of magnetite in magmatic carbonatites (Prins 1972).

It should be noted that these levels of oxygen fugacity are several orders of magnitude higher than the very reduced values (close to the magnetite-wustite buffer) estimated by Prins (1972) for magmatic carbonatites in general (Fig. 3).

The hematite-bearing assemblages must necessarily have equilibrated above the hematite-magnetite buffer.

Stable coexistence of hematite and pyrite is restricted to a narrow, pH-dependent f_{O_2}-interval above the hematite-magnetite buffer (Garrels & Christ 1965, Barnes 1979); at 300°C, the approximate maximum width of this interval amounts to around 3 logarithmic units, which is only attainable at very low pH and high activity of reduced S-species (Helgeson 1969).

At reasonable pH-values (as in a system buffered by calcite), the maximum f_{O_2} of coexisting pyrite and hematite is lower (less than one logarithmic unit above the hematite-magnetite buffer at 300°C). Petrographic evidence suggests that this boundary was also crossed during oxidation of the hematite ore.

Unfortunately, the ores give no evidence as to the maximum f_{O_2} or the temperature of the oxidation process. Because the temperature at which the change from 'reducing' to 'oxidizing' conditions took place cannot be estimated from the present data, several arbitrarily chosen but possible paths of evolution are indicated in Fig. 3.

Sulphide reactions and dissolved sulphur-species distributions

The presence of pyrite in equilibrium with magnetite in the primary magnetite-ores suggests that reduced sulphur species were present in the hydrothermal solutions during primary introduction of the ores, where they may have acted as important complexing agents for iron (Helgeson 1969).

At the maximum stability limit of coexisting hematite and pyrite the equilibria:

(c): $S^{2-} + 2O_2 = SO_4^{2-}$

(d): $H_2S + 2O_2 = HSO_4^- + H^+$

(e): $S_2 + 2H_2O + 3O_2 = 2HSO_4^- + 2H^+$

which determine the distribution of dissolved sulphur species, are all displaced towards the oxidized species (see appendix for thermodynamic relations).

The breakdown of pyrite at high oxygen fugacities, as observed in the Fen ores, therefore produces hematite and an oxidized sulphur-species. The reaction:

(f): $2FeS_2 + 4H_2O + 15/2\ O_2 = Fe_2O_3 + 4SO_4^{2-} + 8H^+$

(or its equivalents involving less dissociated sulphate species) describes the process taking place within the ore system. As no secondary sulphates (gypsum, anhydrite, barite etc.) have been observed in any of the ore samples, the sulphate-ion produced was probably removed from the ores by the hydrothermal fluid.

The hydrogen ions were either consumed by buffer equilibria in the hydrothermal system or were removed as an acidic solution.

pH–buffering of the hydrothermal fluid

A hydrothermal fluid flowing through a carbonate rock is likely to be pH-buffered by equilibria involving wall-rock carbonate and fluids, the simplest of which is:

(g): $CaCO_3 + 2H^+ = Ca^{2+} + H_2O + CO_2$, where solid calcite acts as the proton acceptor, and is *dissolved* to consume excess H^+ – ions introduced into the system. The fluid itself, if isolated from the carbonatite host rock, would have much poorer buffering capacity (which would depend only upon low concentration dissolved species), and would therefore respond to an input of H^+ ions by a decrease of pH. However, efficient shielding of the fluid from the carbonatite is likely to take place only in massive ores or in flow channels bordered by massive ore.

Input of hydrogen ions into the buffered hydrothermal system, e.g. from oxidation of a pyrite-bearing ore, would therefore lead to dissolution of solid carbonate. In a disseminated ore, buffering would take place locally, whereas in calcite-poor massive ore, the ore-wallrock interface is the most probable place for buffering (and calcite dissolution) to take place. This could account for the gradual transition between hematite ore and hostrock, and for the existence of disseminated intermediates between carbonatite and hematite ore sensu strictu.

The mobility of ferric iron in a hydrothermal system is determined by solution equilibria involving hematite or ferric hydroxides, which are all pH-dependent.

To dissolve hematite, pH-values several units below the level of the buffer equilibrium (g) are needed (Garrels & Christ 1966). This limits the solubility of ferric iron during oxidation of the secondary ore to a few ppm, which is too low to explain the abundant hematite found by introduction at high oxygen fugacities, as was suggested by Sæther (1957).

Possible sources of hydrothermal fluids

The ore-evolution at Fen implies a prolonged period of hydrothermal activity, after the intrusion and crystallization of the major carbonatite units. The hydrothermal fluids could either be derived from cooling intrusive rocks, such as the carbonatites themselves, or the major ultramafic silicate intrusive underlying the complex (Ramberg 1973), or be convecting groundwater, driven by heat from cooling intrusives at depth. Sr-isotope data (Andersen in prep.) show that hematite-dolomite-calcite carbonatite (rødberg) surrounding hematite ore is enriched in radiogenic ^{87}Sr relative to other carbonatite units in the complex. This strongly supports a groundwater origin for the late, oxidizing hydrothermal fluids, whereas the provenance of the fluids producing the primary ore remains uncertain.

Conclusions

Iron ores in the Fen complex fall in two main groups: primary magnetite ores and secondary hematite ores. The former group, spatially associated with søvite and rauhaugite, was hydrothermally introduced at temperatures below 600°C, and relatively high oxygen fugacities (between the pyrrhotite-pyrite-magnetite and the hematite-magnetite buffers).

Secondary hematite ores formed by oxidation of pre-existing magnetite ores. Breakdown of pyrite at high f_{O_2} could lead to local hematite enrichment by selective dissolution of carbonates. The chemical evolution of these ores is similar to that of the rødberg host rock.

The major physical factor governing this process is an increase of the oxygen fugacity relative to the hematite-magnetite buffer, with time. This displaces the distribution of dissolved sulphur species towards HSO_4^- and SO_4^{2-} and limits the solubility of iron in the hydrothermal fluid severely. Details of the actual T-f_{O_2} path followed by the hydrothermal fluid are not known, but a simultaneous temperature decrease, due to the influx of groundwater from surrounding gneisses, is the most probable mechanism.

Appendix

Thermodynamical calculations

Only very simple thermodynamic calculations are needed to understand the physicochemical evolution of the ore-system at Fen. In the following paragraph equilibria governing phase stability, oxygen fugacity and dissolved species distribution are calculated in terms of equilibrium constants.

No numerical values are given, as these can easily be obtained from the data sources cited.

No attempts to evaluate deviations from ideality of any of the phases or dissolved species involved are made.

Oxygen fugacity was calculated as a function of temperature for the hematite-magnetite (HM), magnetite-wustite (MW) and graphite – CO–CO_2 (GCC) buffers from equations given by Haggerty (1976) and Wones & Gilbert (1982).

The magnetite – pyrite – pyrrhotite oxygen buffer is defined by the reaction:

(h) $6\,FeS + 2O_2 = Fe_3O_4 + 3\,FeS_2$.

The equilibrium constant of this reaction ($\log K_h = -2 \log f_{O_2}$) was calculated as a function of temperature from thermodynamic data of Helgeson et al. (1978) by the computer program SUPCRT (Kirkham et al. 1978), on the University of Oslo DEC-10 computer.

The oxygen fugacity obtained is the *minimum* at which pyrite and magnetite are stable together. A change of pH towards lower values would increase the actual equilibrium f_{O_2}, and decrease the width of the field of possible coexistence of pyrite and magnetite accordingly. In the presence of pyrite and magnetite, the sulphur- and oxygen fugacities do not vary independently, but are related by the equilibrium:

(i) $3\,FeS_2 + 2O_2 = Fe_3O_4 + 3S_2$, at equilibrium: $\log K_i = 3 \log f_{S_2} - 2 \log f_{O_2}$.

Likewise, equilibrium constants for reactions (a) and (b) limiting the stability field of siderite in the presence of hematite or magnetite were calculated from the data of Helgeson et al. (1978). Assuming the oxide phases involved to be pure and stoichiometric, the equations are simplified to:

$\log K_a\,(T) = 3 \log P_{CO_2} - 1/2 \log f_{O_2}$ below HM
$\log K_b\,(T) = 2 \log P_{CO_2} - 1/2 \log f_{O_2}$ above HM

At any given P_{CO_2}, these equations define curves in the T–f_{O_2} plane that intersect at the HM buffer. In Fig. 3, curves are plotted at 1 bar, 10 bars and 100 bars. The high T, low f_{O_2} limit of the siderite field is practically given by the GCC buffer, below which P_{CO_2} is greatly reduced (French 1971). At the temperatures involved, the

GCC buffer falls within the magnetite stability field.

Equilibrium constants for the reactions controlling sulphur-species distribution (c, d, e) are given by:

$$\log K_c = \frac{a_{SO_4}^{2-}}{a_S^{2-}} - 2 \log f_{O_2}$$

$$\log K_d = \frac{a_{HSO_4^-}}{a_{H_2S}} - 2 \log f_{O_2} - pH$$

$$\log K_e = -3 \log f_{O_2} - \log f_{S_2} + 2 \log a_{HSO_4^-} - 2pH$$

and are listed by Helgeson (1969). The oxygen fugacity, at which $\frac{a_{HSO_4^-}}{a_{H_2S}} = 1$,

at pH buffered by equilibrium (g) ($a_{Ca}^{2+} = 10^{-2}$, $P_{CO_2} = 10$ bar, $P_{tot} = 100$ bar) is plotted in Fig. 3.

pH in a system buffered by calcite (g) is given by the equilibrium constant:

$$\log K_g (T) = \log a_{Ca}^{2+} + \log P_{CO_2} + 2pH$$

which was calculated as a function of temperature at 100 bars from the data of Helgeson et al. (1978). As is seen from the expression, the actual pH of the system is influenced by the activity of calcium in solution and the partial pressure of CO_2. For convenience, a set of arbitrarily chosen values ($a_{Ca}^{2+} = 10^{-2}$ molar, $P_{CO_2} = 10$ bar) has been used in the present calculations.

A change of two orders of magnitude in any of these parameters, would cause a corresponding change in pH by one unit.

Acknowledgements. – I wish to thank K. Mørk for introducing me to the Fen central complex, and H. Qvale and W. L. Griffin for discussions and helpful comments. Samples from the Brøgger collection were made accessible by Mineralogisk-Geologisk Museum, University of Oslo.

Manuscript received January 1983, revised May 1983

References

Andersen, T. 1982: Postmagmatisk utvikling av karbonatittene i Fensfeltet. (abstract) *Geolognytt 17,* 11.

Barth, T. F. W. and Ramberg, I. B. 1966: The Fen circular complex. *in:* Tuttle, O. F. and Gittins, J. (eds.): *Carbonatites,* Interscience, 225–257.

Bjørlykke, H. and Svinndal, S. 1960: The carbonatite and peralkaline rocks of the Fen area. Mining and exploration work. *Nor. geol. unders. 208,* 105–110.

Brøgger, W. C. 1921: Die Eruptivgesteine des Kristianiagebietes: IV. Das Fengebiet in Telemark, Norwegen. *Vit. selsk. skr. I Mat-Nat. Klasse 1920* no. 9, Kristiania.

Dahlgren, S. 1978: Nordagutu, berggrunnsgeologisk kart 1713 IV, M: 1:50 000. Foreløpig utgave. *Nor. geol. unders.*

French, B. M. 1971: Stability relations of siderite ($FeCO_3$) in the system Fe-C-O. *Am. J. Sci. 271,* 37–78.

Garrels, R. M. and Christ, C. L. 1965: *Solutions, Minerals and Equilibria.* Freeman, Cooper & Co. San Francisco. 450 p.

Haggerty, S. E. 1976: Opaque Mineral Oxides in Terrestrial Igneous Rocks. *In* Rumble, D. (ed.): *Oxide Minerals,* MSA Short Course Notes (Reviews in Mineralogy) vol. 3.

Heinrich, E. Wm. 1966: *The Geology of Carbonatites.* 555 p, Rand McNally & Co., Chicago.

Helgeson, H. C. 1969: Thermodynamics of hydrothermal systems at elevated temperatures and pressures. *Am. J. Sci. 267,* 729–804.

Helgeson, H. C., Delany, J. M., Nesbitt, H. W. and Bird, D. K. 1978: Summary and critique of the thermodynamic properties of rockforming minerals. *Am. J. Sci. 278A,* 229 p.

Kirkham, D. H., Walther, J., Delany, J. and Flowers, G. 1978: Computer program SUPCRT. Univ. of California, Berkley.

Lindsley, D. H. 1976: Experimental Studies of Oxide Minerals. *In* Rumble, D. (ed.): *Oxide Minerals,* MSA Short Course Notes (Reviews in Mineralogy) Vol. 3, L61–L84.

Neumann, E. R. 1976: Two refinements for the calculation of structural formulae for pyroxenes and amphiboles. *Nor. Geol. Tidsskr. 56,* 1–6.

Prins, P. 1972: Composition of magnetite from carbonatites. *Lithos 5,* 227–240.

Ramberg, I. B. 1973: Gravity studies of the Fen Complex, Norway, and their petrological significance. *Contr. Mineral. and Petrol. 38,* 115–134.

Sæther, E. 1957: The alkaline rock province of the Fen area in southern Norway. *Det Kgl. N. Vidensk. Selsk. Skr. 1957,* nr 1, 148 p.

Uytenbogaardt, W. & Burke, E. A. J. 1971: *Tables for microscopic identification of ore minerals* 2. revised ed. 430 p. Elsevier.

Vogt, J. H. L. 1918: Jernmalm og Jernverk. *Nor. geol. unders. 85.*

Wones, D. R. and Gilbert, M. C. 1982: Amphiboles in the igneous environment. *In* Veblen, D. R. (ed.): *Reviews in Mineralogy vol. 9B,* 355–390. Mineralogical Society of America.

Wyllie, P. J. 1966: Experimental studies of carbonatite problems: The origin and differentiation of carbonatite magmas. *In* Tuttle, O. F. and Gittins, J.: *Carbonatites,* Interscience, 311–352.